AEM
Journals.ASM.org

Rerouting Carbon Flux To Enhance Photosynthetic Productivity

Daniel C. Ducat,[a,b] J. Abraham Avelar-Rivas,[a,c] Jeffrey C. Way,[b] and Pamela A. Silver[a,b]

Department of Systems Biology, Harvard Medical School, Boston, Massachusetts, USA[a]; Wyss Institute for Biologically Inspired Engineering, Harvard University, Boston, Massachusetts, USA[b]; and Undergraduate Program on Genomic Sciences, National Autonomous University of Mexico, Cuernavaca, Morelos, México[c]

The bioindustrial production of fuels, chemicals, and therapeutics typically relies upon carbohydrate inputs derived from agricultural plants, resulting in the entanglement of food and chemical commodity markets. We demonstrate the efficient production of sucrose from a cyanobacterial species, *Synechococcus elongatus*, heterologously expressing a symporter of protons and sucrose (*cscB*). *cscB*-expressing cyanobacteria export sucrose irreversibly to concentrations of >10 mM without culture toxicity. Moreover, sucrose-exporting cyanobacteria exhibit increased biomass production rates relative to wild-type strains, accompanied by enhanced photosystem II activity, carbon fixation, and chlorophyll content. The genetic modification of sucrose biosynthesis pathways to minimize competing glucose- or sucrose-consuming reactions can further improve sucrose production, allowing the export of sucrose at rates of up to 36.1 mg liter^{-1} h illumination^{-1}. This rate of production exceeds that of previous reports of targeted, photobiological production from microbes. Engineered *S. elongatus* produces sucrose in sufficient quantities (up to ~80% of total biomass) such that it may be a viable alternative to sugar synthesis from terrestrial plants, including sugarcane.

Advances in microbe engineering for the production of biofuels, chemicals, and therapeutics have spurred investment in the production of a wide variety of commodities from biological sources (42). Heterotrophic microbes comprise the vast majority of microorganisms currently utilized for product generation and require a carbohydrate source for carbon and energy that can account for a significant proportion (≤60%) of input costs (24). Such carbohydrate feedstocks are typically derived from agricultural crops, primarily sugarcane, sugar beet, and corn, although lingocellulosic materials are under extensive investigation as alternative feedstocks (33). While biologically produced fuels and chemicals hold the promise of increased sustainability and reduced CO_2 footprints, current feedstock sources place biotechnological processes in competition with agricultural crop lands and food markets. The development of biological alternatives to standard petroleum-based fuels and chemicals has therefore been criticized for its capacity to increase food cost and instabilities (37). Indeed, in recent years sugar prices have increased and fluctuated greatly in global food, driven in part by increased demands for biofuel production (2).

Photosynthetic microorganisms (cyanobacteria and algae) have been proposed as alternative sources for the creation of biofuel-like compounds or industrial feedstocks (27), in part because they possess many advantages over traditional terrestrial plants with regard to targeted metabolite production. For example, the photosynthetic efficiency of cyanobacteria is up to an order of magnitude higher than that of plants (43, 44), and cyanobacteria do not require support tissues that further reduce productive output (e.g., roots/stems). Cyanobacteria are genetically tractable, allowing for rapid engineering and the selection of desirable strains. Finally, cyanobacteria are aquatic microbes with minimal nutritional requirements and can therefore be cultivated in locations that do not compete with traditional agricultural crops. While cyanobacteria and algae share many similar features in this context, the use of algal species for biofuel feedstocks has been explored in much greater detail, partly because of their relatively high lipid content (31), although many cyanobacterial species feature relative simplicity and higher growth rates. Only a small number of reports have been published on the extraction of homogenous, simple carbohydrates from cyanobacterial species (21, 22).

Sucrose is a naturally generated compatible solute synthesized by many cyanobacteria and plants (15), and it is tolerated at high concentrations without toxic effect. Thus, sucrose is an attractive target for overproduction. Under osmotic stress, the model cyanobacterium *Synechococcus elongatus* PCC 7942 (*S. elongatus*) naturally accumulates cytoplasmic sucrose at up to ~300 mM to balance external osmotic pressure (15, 36). However, in the absence of an efficient means to export a target metabolite, the recovery of cytosolic products represents a significant technical barrier to the economic feasibility of microbially synthesized commodities; for example, cell harvesting and the extraction of lipids from algae can represent up to 30% of total production costs (16).

Carbohydrate transport across cell membranes can be mediated by transporters of the major facilitator superfamily (MFS) (21), which includes sucrose permease (*cscB*) (1). Sucrose permease is a sucrose/proton symporter that can confer sucrose uptake activity specifically by utilizing proton gradients established across the cell membrane of most heterotrophic bacteria (Fig. 1A) (29, 38). In contrast, *S. elongatus* drives biochemical reactions from proton gradients established across internal thylakoid membranes and naturally alkalinizes its environment, whereas most heterotrophs actively acidify their growth media. As a result, the orientation of the cell membrane proton gradient is reversed in *S. elongatus* relative to that of most heterotrophs (Fig. 1B). We examined the function of *cscB* when heterologously expressed in *S.*

Received 20 December 2011 **Accepted** 24 January 2012
Published ahead of print 3 February 2012
Address correspondence to Pamela A. Silver, pamela_silver@hms.harvard.edu.
D.C.D. and J.A.A.-R. contributed equally to this work.

doi:10.1128/AEM.07901-11

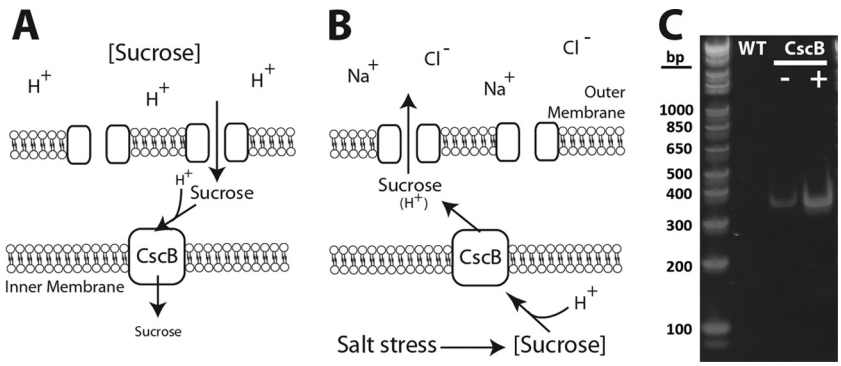

FIG 1 Schematic of sucrose permease activity and expression in *S. elongatus*. (A) Typically, CscB supports sucrose import from relatively acidic environments through proton symport. (B) *S. elongatus* naturally basifies its environment, leading to a reversed proton gradient and CscB directionality. Under hyperosmotic conditions, *S. elongatus* produces cytosolic sucrose for osmotic balance, and it can be exported through the action of CscB. (C) Quantitative reverse transcriptase PCR of the *cscB* transcript in wild-type (WT) and constructed strains with (+) or without (−) IPTG induction.

elongatus to determine its capacity to export cytoplasmically generated sucrose (Fig. 1B).

MATERIALS AND METHODS

Growth conditions and assays. *Synechococcus elongatus* PCC 7942 was grown in temperature-controlled (35°C) and CO_2-controlled (2%) Multitron Infors HT incubators outfitted with 12 18-inch fluorescent bulbs (15 W; Gro-Lux; Sylvania) approximately 35 cm from the culture surface. Light intensity at the growth surface was measured at 65 μE m^2 s^{-1} (LI-250A Light Meter LI-COR with LI-190SA Quantum Sensor or US-SQS Spherical Micro Quantum Sensor; Walz). Flasks were shaken at 150 rpm. Cultures were grown in BG11 medium buffered with 1 g/liter HEPES (pH 8.9; Sigma) to improve consistency during culture dilutions. For yeast coculture experiments, BG11 medium was supplemented with 3 g/liter HEPES (pH 8.9), 1.2 g/liter Difco yeast nitrogen base without amino acids, 1.5 g/liter ammonium sulfate, and 150 mM NaCl (denoted BG11[N]). *Saccharomyces cerevisiae* strain S288c was inoculated in BG11[N] plus 2% sucrose to demonstrate viability in this buffer alone, and the optical density at 600 nm (OD_{600}) was measured every ~20 min on a plate reader (see Fig. 6A). For coculture experiments, *S. elongatus* grown in BG11[N] (OD_{750} of ~1.0) was seeded with *S. cerevisiae* at a concentration of 2×10^5 CFU per ml. Cultures were incubated for 3 days under 35 μE m^2 s^{-1} (ambient temperature and CO_2), and serial dilutions were plated on yeast extract-peptone-dextrose (YEPD) plates to determine yeast viability.

Strain construction and verification. All cloning was conducted using classic restriction/ligation approaches with a BioBrick format (Bgl Brick standard 21) (32) or with isothermal assembly methods (12) in *E. coli* before the transfer of the relevant genetic material to *S. elongatus* through suicide vectors. Sucrose permease (*cscB*) was cloned from *E. coli* genomic DNA (ATCC 700927) and cloned into the neutral site 3 vector under an isopropyl β-D-1-thiogalactopyranoside (IPTG)-inducible promoter (21). *S. elongatus* was transformed overnight in the presence of ~200 ng of this construct, selected on BG11 plates with 12.5 μg/ml chloramphenicol, and verified through PCR/sequencing. Knockout strains were generated through the generation of suicide vectors containing an antibiotic resistance cassette (corresponding to spectinomycin or hygromycin) flanked by *loxP* sites and regions of homology to the genomic site containing the target gene (see Fig. 4B). Invertase (*invA*) mutants were generated through the targeted insertion of a hygromycin resistance cassette (100 μg/ml for selection). ADP-glucose pyrophosphorylase (*glgC*) mutants utilized a spectinomycin cassette (20 μg/ml for selection). Homologous flanking regions of ~1,000 bp were cloned from genomic *S. elongatus* DNA. A pUC57 origin of replication cassette was amplified using the NS3 vector as the template (21). All primers for knockout constructs were designed with either compatible restriction sites or ~20 bp of overlapping sequence, such that isothermal assembly methods (12) could be used to assemble the origin of replication, antibiotic cassette, and flanking homologous sequences into a single vector, which then was transformed into *S. elongatus* as described above. Strains overexpressing glycogen phosphorylase (*glgP*) or UDP-glucose pyrophosphorylase (*galU*) were generated by cloning the relevant gene (from *S. elongatus* or *E. coli* genomic DNA, respectively) into the neutral site 2, IPTG-inducible vector (10) and selecting for double recombinants on BG11 plates supplemented with 20 μg/ml kanamycin.

All strains generated in this study were verified for the incorporation of the relevant DNA into the *S. elongatus* genome through routine colony PCR using multiple primer sets. Strains were further verified for the expression of the appropriate mRNA (or lack of expression of endogenous mRNA with respect to gene knockouts) by reverse transcriptase PCR. Cyanobacterial cells of the appropriate strain were grown in the presence or absence of IPTG as appropriate, and RNA was isolated from each strain through the use of TRIzol-chloroform-isopropanol extraction per the manufacturer's instructions (Invitrogen). Equivalent amounts of RNA were used to generate cDNA using SuperScript III (Invitrogen) per the manufacturer's instructions. Equivalent amounts of resulting cDNA were used as the template in PCRs with multiple primer pairs designed for the amplification of ~200- to 400-bp regions of relevant transcripts (see Fig. 1C and 4C for representative images; a full list of all primers used in this study is available upon request).

Sucrose assays. CscB-expressing cells were grown as described above, and samples were taken from cultures as indicated, with the replacement of removed volume by fresh BG11 of the appropriate osmolarity (0, 50, 100, 150, or 200 mM NaCl). For growth curve experiments, flasks were weighed at the setup of the time course experiments, and water was added prior to each sampling to correct for evaporation rates. CscB-expressing cells were induced with 1 mM IPTG and the indicated salt concentrations. After pelleting cyanobacterial cells, sucrose was measured from the supernatant fraction using sucrose/D-glucose assay kits (Megazyme). Experiments designed to measure the pH dependence of sucrose export (Fig. 2C) were conducted in an open-air incubator, as the formation of bicarbonate from CO_2 dissolution in an enriched headspace prevented the precise control of pH. These cultures were grown up to 48 h at room temperature without shaking at 100 μE m^2 s^{-1} in BG11 plus 2 g HEPES/liter and adjusted to the indicated pH with KOH. Specific productivities of sucrose were determined by the direct measurement of cell numbers in cyanobacterial cultures using a MultiSizer 4 Coulter counter (Beckman Coulter).

Oxygen evolution/chlorophyll content and ^{14}C fixation. For the time course analysis of sucrose production, oxygen evolution, and chlorophyll content, the relevant cyanobacterial cultures were grown in BG11 plus 150 mM NaCl medium and backdiluted to an OD_{750} of 0.3 (SpectraMax M5; Molecular Devices) every 24 h to minimize cell shading and to standardize

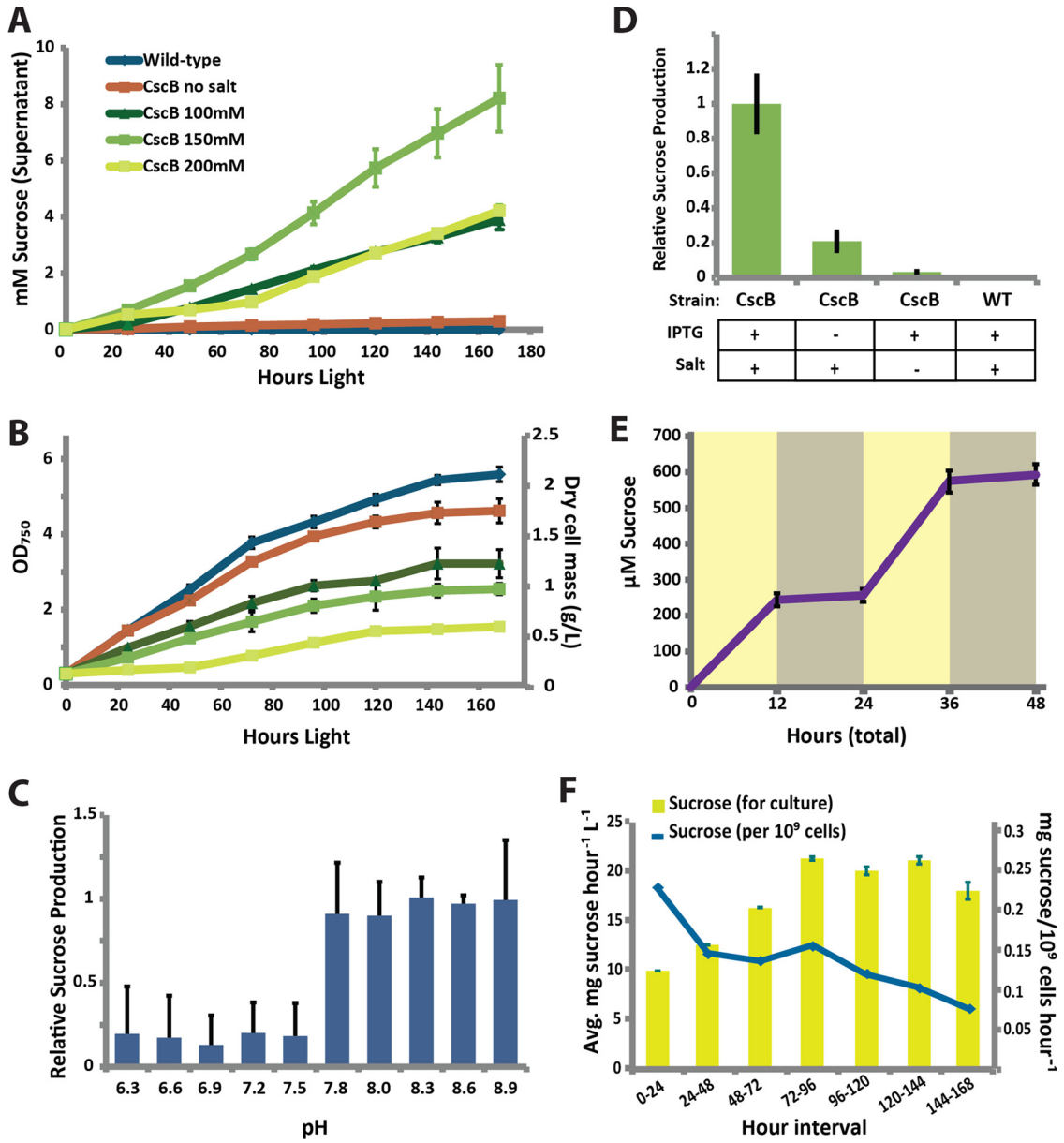

FIG 2 CscB-dependent export of sucrose in growing cyanobacterial cultures. (A) Concentration of sucrose in the supernatant of *S. elongatus* cultures with or without *cscB* expression when grown with 0 to 200 mM NaCl for 1 week in constant light. (B) Cell growth of cultures shown in panel A as measured by optical density at 750 nm (OD_{750}). Sucrose export is dependent upon culture pH (C) and both IPTG and salt induction (D). (E) Sucrose produced by *cscB*-expressing *S. elongatus* under alternating periods of light (yellow) and dark (gray). (F) Daily total (yellow bars) and per-cell (blue line) rate of sucrose production for 150 mM NaCl-induced cultures shown in panel A. Data are from representative experiments where error bars represent standard deviations from ≥3 replicates.

cell density. For the analysis of dry cell mass as shown in Fig. 3, 6 to 10 ml of cyanobacterial culture was pelleted for 30 min at 20,000 × *g*, desiccated in a GeneVac E2-2 Plus evaporator (SP Scientific), and weighed. Dry weight values displayed in Fig. 2B are estimated from the OD_{750} based on a standardized curve. Dissolved oxygen and chlorophyll content were measured on 2 ml of backdiluted (OD_{750} of 0.3) cultures with the use of Clark electrodes (model 1302; Strathkelvin) outfitted with polypropylene membranes and monitored with a 782 dual-channel oxygen meter (Strathkelvin). Cyanobacterial cultures were contained in transparent, water-jacketed respiration cells (RC350; Strathkelvin), illuminated with constant light (35 μE m^2 s^{-1}; white fluorescent), and continuously stirred. Constant temperature (22°C) was maintained throughout the length of each oxygen measurement (10 min) through water exchange in the respiration cell jacket and with an external fan. Chlorophyll was extracted from cyanobacterial cells using 85% methanol with 1 mM sodium dithionite, and the concentration was determined as previously described (25). Wild-type *S. elongatus* cultures in normal medium (i.e., not exposed to salt stress) exhibited oxygen evolution capacity and growth rates similar to those of wild-type strains acclimatized to 150 mM NaCl.

Carbon uptake experiments were performed from backdiluted cultures of wild-type or *cscB*-induced strains of *S. elongatus* as described above. Cultures were backdiluted for at least 4 successive days to allow for the acclimatization of *cscB*-expressing cells as described for Fig. 3C. Radiolabeled [^{14}C]sodium bicarbonate (3 μl of 1 mCi/ml; 52.0 mCi/mmol; Perkin Elmer) was added to 3 ml of wild-type or *cscB*-expressing cells, whereupon cells were incubated at room temperature under 65 μE m^2 s^{-1}

illumination for 10 min. Reactions were terminated via the addition of 100 μl glacial acetic acid. Fixed ^{14}C was measured with a scintillation counter (LS 6500; Beckman Coulter).

Calculations comparing cyanobacterial sucrose productivity. In surveying the literature, we came across substantial variation in the assumptions used to model potential biomass yield from cyanobacteria or algae. Since relatively limited information is available on the design or productivities of scaled, enclosed photobioreactors, we used numbers from meta-analyses of microalgal production models (for both open and closed reactors) (9, 28) to calculate a high (volumetric) and low (areal) theoretical upper yield of scaled sucrose production from *S. elongatus*. Using the volumetric productivities we achieved under laboratory conditions (36.1 mg liter^{-1} h^{-1}), which were scaled to a 1-ha photobioreactor with a volume of 640,000 liters (9), a median growing season of 300 days (28), and 8 h of light per day, we calculate a theoretical yield of ~55 metric tons of sucrose per hectare per year. Estimating yields from areal productivities achieved under laboratory conditions (50-ml cultures in 150-ml flasks, with a bottom surface area of ~0.002826 m^2; 637 mg m^{-2} h^{-1}) and using median values for growing season (300 days), 8 h of light per day, and 86.7% coverage of photobioreactor (28), we estimate a yield of ~15 metric tons sucrose per hectare per year. We note that the ~4-fold difference between these calculations is largely a function of the underestimation of potential areal productivities from our small-scale cultivars (which are grown at depths of only ~2 cm) under relatively low light intensities (~10-fold less than full sunlight).

In comparing our sucrose export rates to a patented acid-wash technique (22), we estimate that *cscB*-mediated sucrose transport can be up to 30 times more effective (36 mg/liter sucrose h^{-1} × 12 h day^{-1} × 7 days = ~3,000 mg sucrose). Data presented in Table 2 of the relevant patent (22) shows the extraction of 110.5 mg/liter sucrose from 1 week's growth of *S. elongatus* in a 12-h day, 12-h night light regimen.

RESULTS AND DISCUSSION

CscB-dependent export of sucrose. We cloned *cscB* from *Escherichia coli* and integrated it into a genomic neutral site of *S. elongatus* under an IPTG-inducible promoter (21). We determined that *cscB* gene transcripts were expressed using reverse transcription-PCR (RT-PCR) and quantified an ~6-fold induction of *cscB* transcript levels in the presence of 1 mM IPTG (Fig. 1C).

When heterologously expressed in *S. elongatus*, CscB allows the export of cytoplasmic sucrose generated in response to osmotic shock (Fig. 2). CscB-expressing cyanobacteria exposed to 100 to 200 mM NaCl steadily export sucrose into the culture supernatant when grown in constant light in the presence of 1 mM IPTG, whereas sucrose export is undetectable in wild-type cultures (Fig. 2A). The rate of sucrose export is influenced by a number of factors, including the degree of osmotic pressure applied to the culture, and is inversely correlated with cyanobacterial growth (Fig. 2B). Furthermore, sucrose export rates exhibit a biphasic pattern dependent upon medium pH, with maximal sucrose export observed above pH 7.8, which is consistent with the sucrose/proton symport activity of CscB (Fig. 2C). The rate of sucrose export also depends on both osmotic pressure and IPTG induction (Fig. 2D). Sucrose export is light dependent, accruing during the lighted periods of cultures grown under alternating periods of day and night (12 h/12 h light/dark) (Fig. 2E); no net reuptake of sucrose is observed in the dark. Total sucrose production rates of a growing culture increase as cyanobacterial cultures age and become more dense (Fig. 2F), distinguishing sucrose production from other reported forms of photobiological production which frequently exhibit feedback inhibition through product toxicity or backpressure (3, 11, 11a). Although total sucrose production increases in more dense cyanobacterial cultures, the specific productivity of sucrose declines (Fig. 2F), as is expected due to light limitation caused by cell shading.

Since exported sucrose represents fixed carbon that is diverted from cell growth processes (Fig. 2B and 3A), one measure of the productive capacity of engineered sucrose-exporting cyanobacteria is comparing the potential cellular biomass that is accumulated in the absence of *cscB* expression to biomass in its presence. We monitored the production of cyanobacterial biomass (dry weight) and sucrose biomass 24 h following *cscB* induction in cells preacclimated to BG11 with no added salt (Fig. 3A) or BG11 with 150 mM NaCl (Fig. 3B) and compared productivities to those of uninduced and wild-type cultures. *cscB*-induced cyanobacteria accumulated less cellular biomass than wild-type or uninduced cultures, and the initial biomass of sucrose exported was essentially equivalent to this difference (0 to 24 h) (Fig. 3A and B). Thus, on short time scales, cellular biomass can be exchanged for sucrose biomass with near 100% efficiency. Furthermore, the ratio of cellular biomass to sucrose can be tuned via the osmotic pressure imposed on the cyanobacterial culture, allowing up to ~80% of biomass to be generated as sucrose at higher salinities (200 mM NaCl) (Fig. 3A).

Enhancement of biomass productivity and photosynthetic activity. We followed the productivity of sucrose-exporting cells beyond the first day, diluting cultures to a constant volume and density (114 ± 7 mg/liter) in 150 mM NaCl each day to equilibrate samples and minimize light shading (Fig. 3B). We observed gradual increases in sucrose and cell biomass production in *cscB*-induced cultures over time, resulting in total biomass productivities that were up to 35% greater than the biomass produced by wild-type cultures, as well as sucrose productivities up to ~200% of initial cellular mass in 24 h (Fig. 3B). These heightened levels of productivity were maintained for the length of our observations (2 weeks).

Since *S. elongatus* is a strictly autotrophic species of cyanobacteria, we asked if increased photosynthetic activity could partially explain the increased biomass fixed by *cscB*-expressing cells. We measured oxygen evolution rates of the water-splitting reaction of photosystem II (PSII) and observed gradual increases in the activity of *cscB*-expressing cyanobacteria 48 to 96 h following induction, to final oxygen evolution rates ~20% higher than those of wild-type or uninduced cultures (Fig. 3C). Chlorophyll concentration showed a similar increasing pattern in *cscB*-expressing cyanobacteria (~25%) (Fig. 3D). Finally, we observed a 20% increase in the rate of carbon fixation in *cscB*-expressing cells by monitoring the incorporation of ^{14}C-labeled bicarbonate into organic matter (Fig. 3E). These results indicate that photosynthetic activity is upregulated in *cscB*-expressing *S. elongatus*, which may partially account for the enhancement of photosynthetic productivity observed in this strain (Fig. 3B).

Engineering carbohydrate metabolic pathways for enhanced sucrose production. We next sought to enhance sucrose production in *S. elongatus* by biasing glucose-1-phosphate flux toward sucrose and away from storage as glycogen. Glucose-1-phosphate derived from products of the Calvin cycle is converted to UDP-glucose through the action of UDP-glucose pyrophosphorylase (*galU*) (Fig. 4A). Sucrose is produced from UDP-glucose and fructose via the combined actions of sucrose-phosphate synthase and sucrose-phosphate phosphatase (30); invertase (*invA*) hydrolyzes sucrose to glucose and fructose. Alternatively, glucose can be

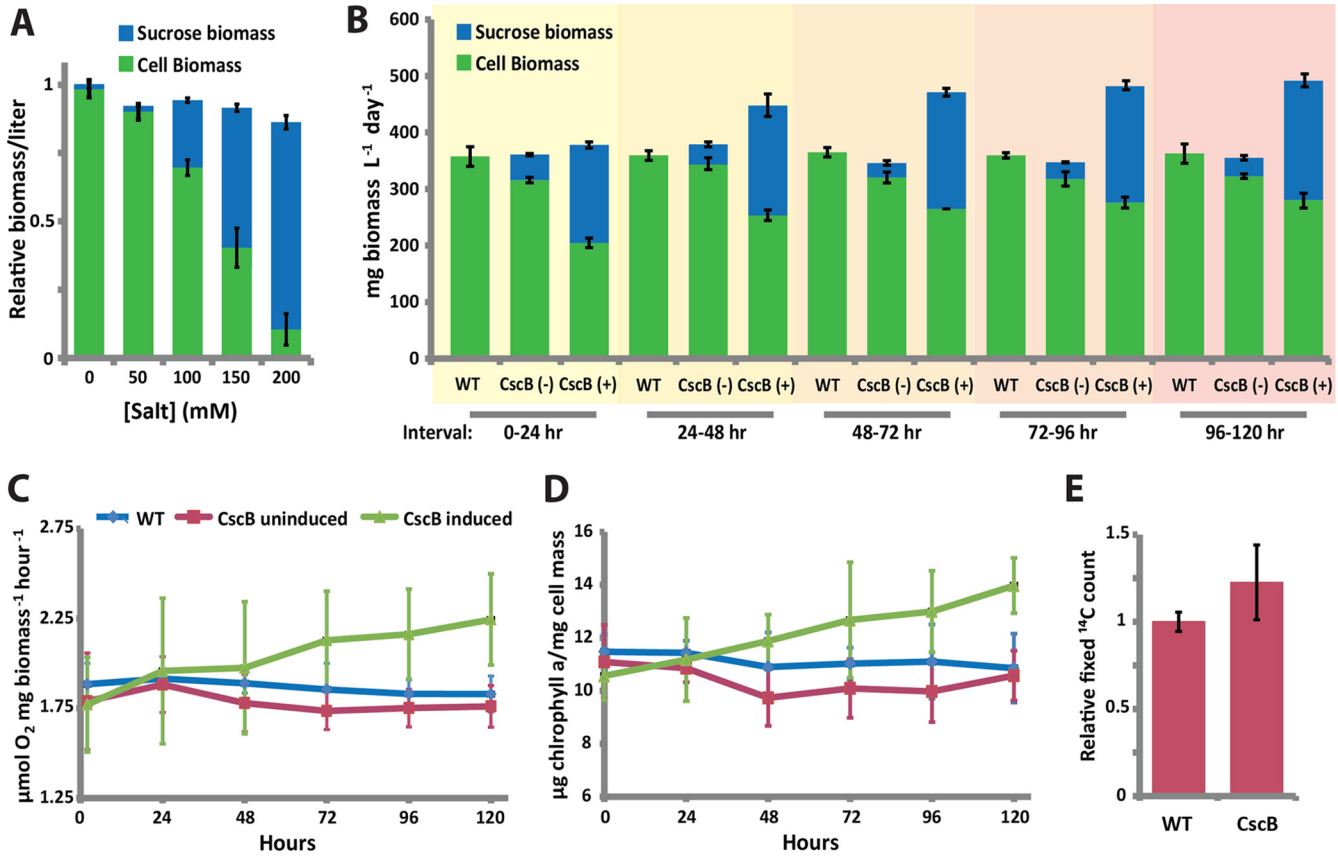

FIG 3 Increased biomass production and photosynthetic activity in *S. elongatus* exporting sucrose. (A) Normalized sucrose and cellular biomass fixed in the first 24 h following transfer to the indicated level of salt. (B) Measurement of cyanobacterially produced cellular biomass (dry weight; green) and sucrose biomass (blue) produced by wild-type (WT), uninduced (−), and *cscB*-expressing (+) strains after 24 h in cultures acclimatized to 150 mM NaCl. The time of 0 h represents the time of initial induction with 1 mM IPTG and where cultures are backdiluted to constant density (114 ± 7 mg cell mass liter^{-1}) at the start of each 24-h cycle. Oxygen evolution rates (C) and chlorophyll *a* contents (D) of wild-type, uninduced, and induced cyanobacterial cultures for cells treated as described for panel B. (E) Relative carbon fixation rates of WT and *cscB*-expressing cells as determined by the incorporation of radiolabeled [^{14}C]bicarbonate, where *cscB*-expressing cultures were induced for at least 4 days and backdiluted to constant density as described for panel B. Data for panels A and B are from a representative experiment where similar results were obtained for at least 5 independent replicates. Data for panels C to E represent averages from ≥4 independent experiments. Error bars indicate standard deviations from ≥3 replicates.

polymerized into glycogen through the sequential activities of ADP-glucose pyrophosphorylase (*glgC*) and glycogen synthase (*glgA*) (Fig. 4A). Glycogen breakdown is regulated by a number of activities, including glycogen phosphorylase (*glgP*). To bias carbon flux toward sucrose production, we generated Δ*invA* and Δ*glgC* strains through the replacement of endogenous genes by homologous recombination (Fig. 4B) and constructed strains overexpressing *glgP* and *galU*. We verified the complete knockout of target genes and the expression of *glgP* and *galU* through the analysis of mRNA transcripts by RT-PCR (representative images are shown in Fig. 4C). All strains generated in this study exhibited lower growth rates than wild-type *S. elongatus*, although the severity of these phenotypes depended on the osmotic pressure of the medium used to culture the cells and whether or not the cells were preacclimatized to a higher osmotic pressure before growth rates were determined (Table 1). The strongest defect in growth was observed following the transfer of *glgC*-deficient cyanobacteria from low-salt to high-salt medium (Table 1), in agreement with previously published results (36).

As predicted, strains deficient for the putative invertase (Synpcc7942_0397) or *glgC* exported sucrose at higher rates (~10 to 15%) (Fig. 4D). The knockout of both *invA* and *glgC* produced additive effects with regard to sucrose export (~25% increase) (Fig. 4D). In contrast, the heterologous expression of *galU* or the overexpression of *glgP* caused a reduction in the rate of sucrose export relative to that of cells expressing *cscB* alone (Fig. 4D). The failure of *glgP*- or *galU*-expressing strains to increase sucrose productivities could be a result of toxicity resulting from overexpression, particularly with regard to *galU*, a strain that exhibited general growth impairments (Table 1) and abnormal pigmentation. Additionally, GlgP activity is posttranslationally regulated (5), and therefore *glgP* overexpression may not have led to an equivalent increase in glycogen breakdown.

Comparison of cyanobacterial sucrose production to other photobiological productivities. The sucrose production rates displayed in Fig. 4D (36.1 mg liter^{-1} h^{-1} for the Δ*invA* Δ*glgC* strain) were derived from mature cultures (~1.15 g dry cell weight liter^{-1}) and were maintained for the duration of our observations (3 days). To our knowledge, this productivity is the highest photosynthetic rate of microbial target product formation reported in academic literature for cyanobacteria or algae (Fig. 5A), and it exceeds (by ~30-fold) that of a previously patented strategy for

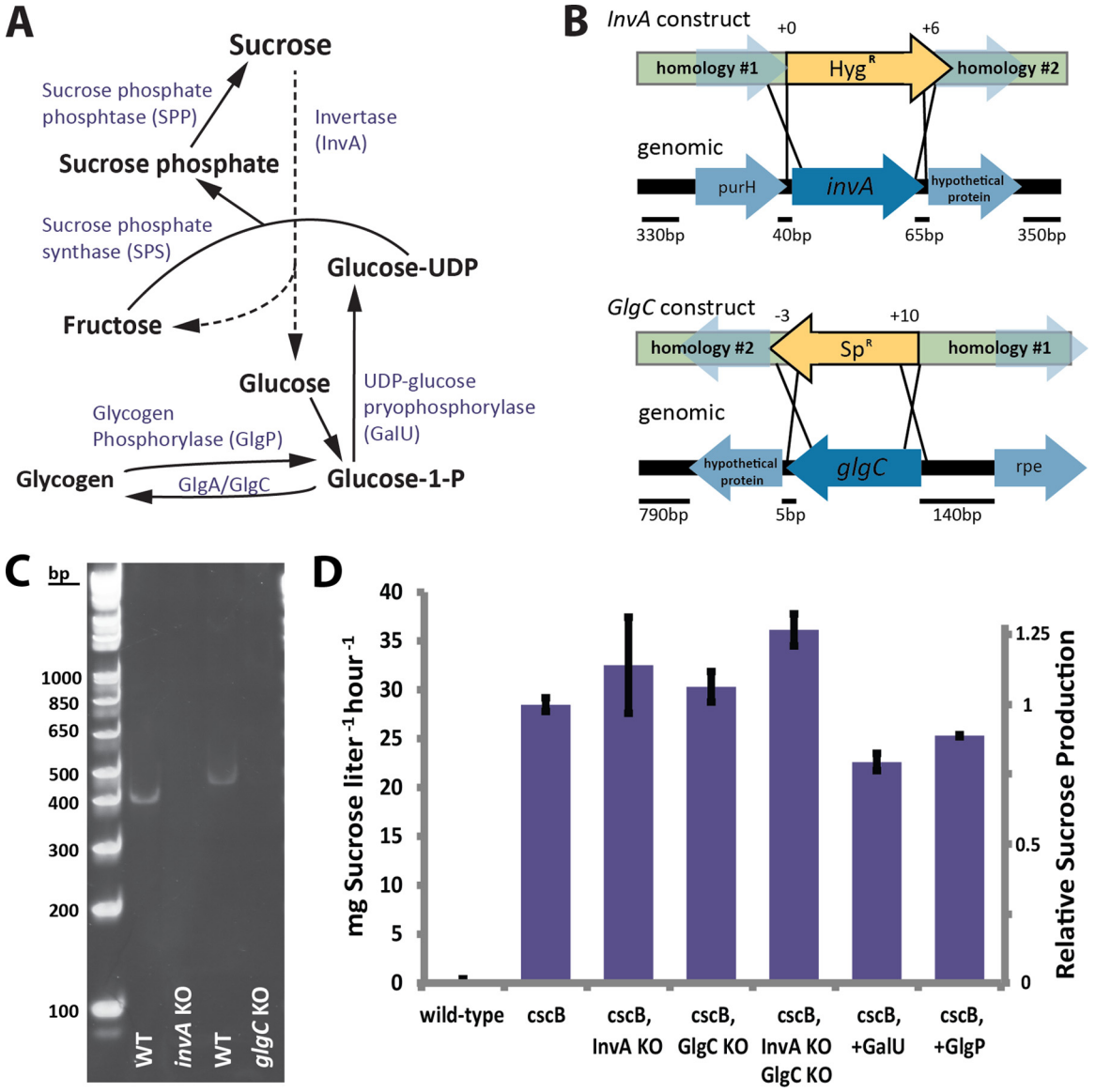

FIG 4 Engineering of glucose metabolism for improved sucrose secretion. (A) Schematic of glucose and sucrose metabolism in *S. elongatus*. (B) Schematic of constructs designed for site-directed elimination of target genes (*invA* and *glgC*) at the depicted loci in *S. elongatus*. Resistance cassettes were flanked by DNA homologous to sequences neighboring target genes to allow for the selection of strains with the loss of target genes following homologous recombination. Any additional/fewer base pairs recombined relative to the start or stop codons of the target gene are indicated above the construct depiction. (C) Representative reverse transcriptase PCRs from the wild-type strain or the indicated knockout strains using primers targeting *invA* or *glgC* transcript (expected size of 410 and 470 bp, respectively). (D) Sucrose production rates for strains of *S. elongatus* with modifications in the indicated sucrose/glucose metabolic genes by knockout (KO) or gene expression (+).

extracting sucrose from cyanobacteria (22). For example, *S. elongatus* has recently been engineered to produce isobutyraldehyde at 6.13 mg liter^{-1} h^{-1} averaged over 1 week (3). Similarly, a number of photosynthetic microbes have been analyzed for their potential to produce biodiesel precursors; bulk lipids are naturally produced at high levels in the algae *Neochloris oleoabundans* (~6.83 mg lipid liter^{-1} h^{-1}) (13, 17), and cyanobacteria have recently been engineered to excrete a mix of fatty acids (~8.2 mg fatty acid liter^{-1} h^{-1}) (Fig. 5A) (19).

Sucrose production in engineered *S. elongatus* compares favorably with sugarcane and other agricultural crops. Sugarcane yields range from 30 to 70 metric tons ha^{-1} year^{-1} (dry weight), depending on location (39 and http://www.nass.usda.gov/). Cyanobacteria or algae cultivated in closed bioreactors generate ~40 to 120 metric tons ha^{-1} year^{-1} in small-scale reactors (8, 14, 20, 26), and open pond designs yield ~25 to 50 metric tons ha^{-1} year^{-1} (16, 28). As the areal productivities of sugarcane and cyanobacteria are similar, the percentage of total biomass generated as sucrose is the simplest comparison between sugarcane (15%) and *S. elongatus* (up to 80%) (Fig. 3B). Although speculative, we also calculated more detailed estimations of cyanobacterial sucrose productivity using median values from meta-analyses of microalgal productivity (see Materials and Methods) (9, 28) to illustrate that *S. elongatus* could

TABLE 1 Growth rates of constructed strains[a]

Strain	Growth rate by salt condition: BG11, no salt	Salt stress (150 mM)	Salt (after acclimatization)
WT	11.5	12.0	12.0
CscB	12.0	14.5	13.0
CscB + IPTG	12.0	19.0	13.5
CscB, GalU	15.0	16.5	15.5
CscB, GalU + IPTG	18.0	20.5	19.0
CscB, InvA	13.5	16.0	14.5
CscB, GlgC	12.5	43.5	20.0
CscB, GlgP	13.0	16.0	15.0
CscB, GlgP + IPTG	15.0	20.0	15.5

[a] Doubling times for the indicated strains when grown under constant light with 2% CO_2. Rates are calculated for growth in normal BG11 medium, immediately following transfer into 150 mM NaCl, and after acclimatization (≥4 days) to high salt (150 mM NaCl). CscB, strain expressing CscB; CscB + IPTG, CscB-expressing strain grown in the presence of IPTG; CscB, GalU, strain expressing CscB and GalU; CscB, InvA, strain expressing CscB and InvA; CscB, GlgC, strain expressing CscB and GlgC; CscB, GlgP, strain expressing CscB and GlgP.

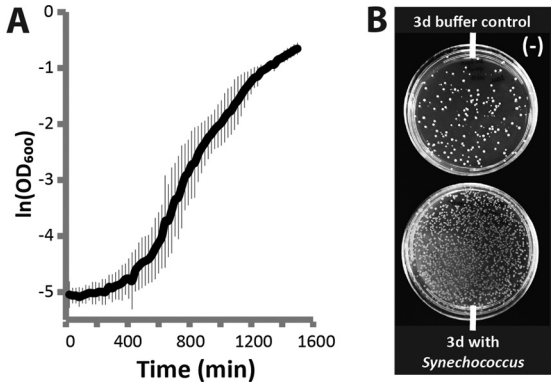

FIG 6 Support of heterotrophic metabolism from cyanobacterially produced sucrose. (A) Growth curve of *S. cerevisiae* incubated alone in BG11[N_2] medium supplemented with 2% sucrose. (B) Yeast viability following 3 days (3d) of growth in BG11[N_2] alone (top) or cocultured with sucrose-exporting cyanobacteria (bottom).

produce sucrose at rates up to severalfold higher than that of sugarcane, assuming the scalability of laboratory results on either a volumetric or areal basis (Fig. 5C).

Heterotrophic metabolism supported by cyanobacterial sucrose. Cyanobacterially derived sucrose could support the biological production of other compounds, including commodity products (e.g., biofuels), where carbohydrate feedstocks represent significant portions of input costs (24). The direct use of cyanobacterial supernatant as a feedstock for bioindustrial microbes could be a particularly promising approach, as it could limit the need to purify/concentrate exported sucrose. We therefore examined the capacity of sucrose-exporting *S. elongatus* to provide a carbon source for the growth of a heterotrophic species. *Saccharomyces cerevisiae* is a well-established heterotrophic microbe of academic and industrial relevance, so we first tested the compatibility of cyanobacterial growth medium with yeast. Using a modified BG11 medium containing additional sources of nitrogen (BG11[N]; see Materials and Methods), we observed normal yeast growth if 2% sucrose was provided as a carbon source (Fig. 6A). We then examined yeast viability when directly cocultured with *cscB*-expressing *S. elongatus*. *S. cerevisiae* (starting density, 2×10^5) incubated 3 days in BG11[N] medium with *cscB*-expressing *S. elongatus* underwent ~2 doublings (final viable count, 8.1×10^5), while viability decreased in a BG11[N]-only control (final viable count, 8.5×10^4) (Fig. 6B). Thus, sucrose-exporting *S. elongatus* can directly supply a usable energy source to another commercially relevant organism.

The enhancement of PSII activity, chlorophyll concentration, and carbon fixation is a striking feature of engineered, sucrose-

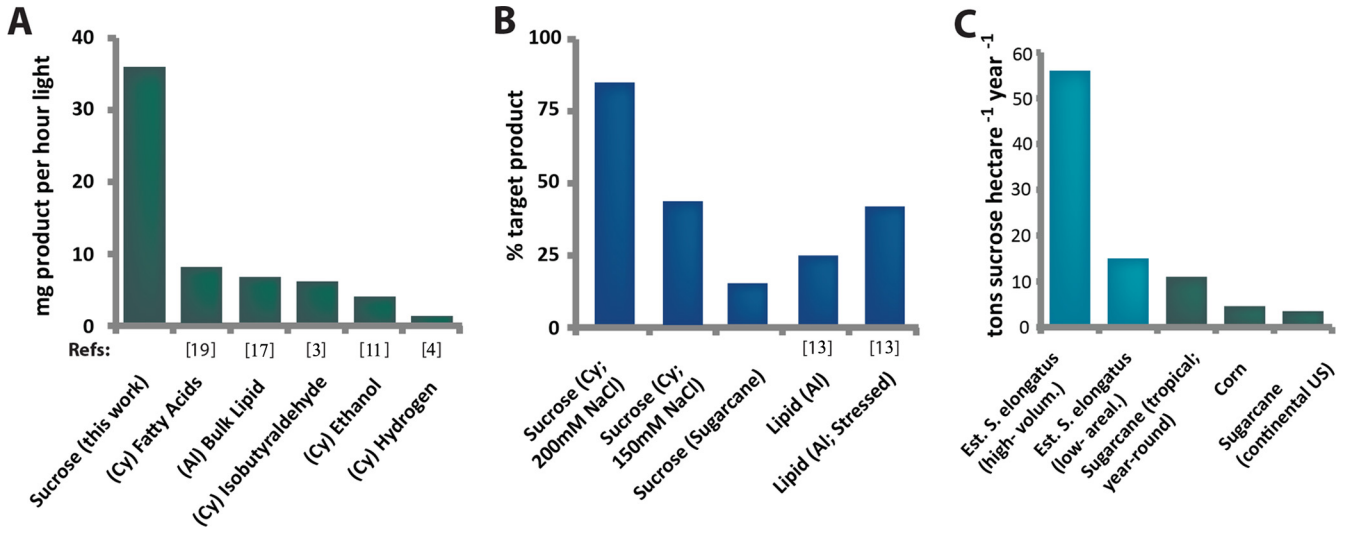

FIG 5 Comparison of cyanobacterial sucrose productivity to alternative photobiological productivities. (A) Summary of photobiological product formation rates from existing literature on cyanobacteria (Cy) and algae (Al). (B) Sucrose productivity in *cscB*-expressing *S. elongatus* compares favorably to the percentage of total biomass directed to named metabolites for example species. (C) Estimated potential of sucrose production from scaled cultures of *cscB*-expressing *S. elongatus* using volumetric (high) and areal (low) productivities obtained under laboratory environmental conditions (blue; see Materials and Methods for details). Known carbohydrate productivities for traditional terrestrial crops are plotted for comparison (green) (34, 39; also http://www.nass.usda.gov/). The sources of other data are indicated beneath the bars (3, 4, 11, 13, 17, 19).

exporting cyanobacteria (Fig. 3). In a natural context, sucrose and other compatible solutes affect cellular physiology through multiple mechanisms. For example, under stress conditions sucrose may have direct protective functions (e.g., enhancing membrane integrity), provide an easily accessible energy source, have antioxidant properties, act as a balancing osmolyte, and/or have signaling functions (15, 40). Furthermore, the production of sugars consumes excess reducing equivalents and triose phosphate intermediates, which can alleviate the inhibition of photosynthetic activity (photoinhibition) resulting from energy imbalances between light absorption (source) and metabolic capacity (sink) (18, 23, 40). Indeed, transient increases in photosynthetic activity of other freshwater cyanobacterial species exposed to osmotic stress have been reported but are restricted to a period of cytosolic sucrose accumulation (~2 days) (6, 7).

We propose that CscB-supported sucrose export provides an expanded photosynthetic sink, helping maintain a relatively oxidized electron transport chain and suppressing photoinhibition, analogously to plants with large carbon sinks (e.g., potatoes) (23). We note that while any concentration-dependent protective effects of sucrose would be diluted in *cscB*-expressing cells, the continual replacement-level synthesis of sucrose could maintain an altered metabolic state that is associated with sucrose production. The increased PSII activity, chlorophyll content, and carbon fixation we observe in sucrose-exporting cyanobacteria (Fig. 3C to E) are consistent with a relaxation of photoinhibition, a common feature of cyanobacterial growth under photobioreactor-like conditions (23, 35).

As photosynthetic organisms have evolved a light-gathering ability in excess of metabolic processing capacity under full illumination, the optimization of source/sink balance is necessary to minimize photosynthetic inefficiencies (43). The limitation of light capture capacity has received considerable attention following reports of algae with reduced chlorophyll antennae and improved productivity (20). However, there are no previous reports of metabolite production and export that have led to enhancements in photosynthetic yield from microbes, although some plants exhibit complex phenotypes, including increased productivity upon the expansion of carbohydrate sinks (23, 41), and cyanobacteria engineered to excrete fatty acids exhibit enhanced viability under specific, photobioreactor-like environments (high light and high CO_2) (19). The expansion of cellular metabolic sinks represents an alternative, complementary balancing strategy that may be generalizable to multiple photosynthetic products to bring photosynthetic productivity closer to maximal theoretical yields (43).

ACKNOWLEDGMENTS

A special thanks to Ilan Wapinski for valuable assistance with yeast strains and coculture experiments. We thank members of the Silver laboratory for helpful discussions and the critical review of the manuscript.

We acknowledge funding from the National Institute of General Medical Sciences, award number F32GM093516, Army Research Office award no. W911NF-09-1-0226, DOE ARPA-E award DE-0000079 Cooperative Agreement, the Wyss Institute for Biologically Inspired Engineering, SEP-DGRI, Mexico, and the agreement between CCG and Fundacion Mexico en Harvard A.C.

One author (J.C.W.) holds the following patent, which is applicable to cyanobacterial sucrose production: WO2011029013.

REFERENCES

1. **Abramson J, Iwata S, Kaback HR.** 2004. Lactose permease as a paradigm for membrane transport proteins (review). Mol. Membr. Biol. **21**:227–236.
2. **Anonymous.** 2011, posting date. World food situation. Food and Agriculture Organization of the United Nations http://www.fao.org/worldfoodsituation/wfs-home/en/.
3. **Atsumi S, Higashide W, Liao JC.** 2009. Direct photosynthetic recycling of carbon dioxide to isobutyraldehyde. Nat. Biotechnol. **27**:1177–1180.
4. **Bandyopadhyay A, Stockel J, Min H, Sherman LA, Pakrasi HB.** 2010. High rates of photobiological H2 production by a cyanobacterium under aerobic conditions. Nat. Commun. **1**:139.
5. **Barford D, Hu SH, Johnson LN.** 1991. Structural mechanism for glycogen phosphorylase control by phosphorylation and AMP. J. Mol. Biol. **218**:233–260.
6. **Blumwald E, Mehlhorn RJ, Packer L.** 1983. Ionic osmoregulation during salt adaptation of the cyanobacterium Synechococcus 6311. Plant Physiol. **73**:377–380.
7. **Blumwald E, Tel-Or E.** 1982. Osmoregulation and cell composition in salt-adaptation of Nostoc muscorum. Arch. Microbiol. **132**:168–172.
8. **Brennan L, Owende P.** 2010. Biofuels from microalgae–a review of technologies for production, processing, and extractions of biofuels and coproducts. Renew. Sustain. Energy Rev. **14**:557–577.
9. **Chisti Y.** 2008. Biodiesel from microalgae beats bioethanol. Trends Biotechnol. **26**:126–131.
10. **Clerico EM, Ditty JL, Golden SS.** 2007. Specialized techniques for site-directed mutagenesis in cyanobacteria. Methods Mol. Biol. **362**:155–171.
11. **Dexter J, Fu P.** 2009. Metabolic engineering of cyanobacteria for ethanol production. Energy Environ. Sci. **2**:857–864.

11a. **Ducat DC, Sachdeva G, Silver PA.** 2011. Rewiring hydrogenase-dependent redox circuits in cyanobacteria. Proc. Natl. Acad. Sci. U.S.A. **108**:3941–3946.

12. **Gibson DG, et al.** 2009. Enzymatic assembly of DNA molecules up to several hundred kilobases. Nat. Methods **6**:343–345.
13. **Griffiths M, Harrison S.** 2009. Lipid productivity as a key characteristic for choosing algal species for biodiesel production. J. Appl. Phycol. **21**:493–507.
14. **Huntley M, Redalje D.** 2007. CO2 mitigation and renewable oil from photosynthetic microbes: a new appraisal. Mitigation Adapt. Strategies Global Change **12**:573–608.
15. **Klahn S, Hagemann M.** 2011. Compatible solute biosynthesis in cyanobacteria. Environ. Microbiol. **13**:551–562.
16. **Kovacevic V, Wesseler J.** 2010. Cost-effectiveness analysis of algae energy production in the EU. Energy Policy **38**:5749–5757.
17. **Li Y, Horsman M, Wang B, Wu N, Lan CQ.** 2008. Effects of nitrogen sources on cell growth and lipid accumulation of green alga Neochloris oleoabundans. Appl. Microbiol. Biotechnol. **81**:629–636.
18. **Li Z, Wakao S, Fischer BB, Niyogi KK.** 2009. Sensing and responding to excess light. Annu. Rev. Plant Biol. **60**:239–260.
19. **Liu X, Sheng J, Curtiss R, III.** 2011. Fatty acid production in genetically modified cyanobacteria. Proc. Natl. Acad. Sci. U. S. A. **108**:6899–6904.
20. **Melis A.** 2009. Solar energy conversion efficiencies in photosynthesis: minimizing the chlorophyll antennae to maximize efficiency. Plant Sci. **177**:272–280.
21. **Niederholtmeyer H, Wolfstadter BT, Savage DF, Silver PA, Way JC.** 2010. Engineering cyanobacteria to synthesize and export hydrophilic products. Appl. Environ. Microbiol. **76**:3462–3466.
22. **Nobles DR.** October 2007. Production and secretion of sucrose in photosynthetic prokaryotes (cyanobacteria). US patent 2008/0124767 A1.
23. **Paul MJ, Foyer CH.** 2001. Sink regulation of photosynthesis. J. Exp. Bot. **52**:1383–1400.
24. **Pimentel D, Patzek TW.** 2008. Ethanol production: energy and economic issues related to U.S. and Brazilian sugarcane biofuels. Springer, Amsterdam, Netherlands.
25. **Porra RJ.** 2002. The chequered history of the development and use of simultaneous equations for the accurate determination of chlorophylls a and b. Photosynth. Res. **73**:149–156.
26. **Posten C.** 2009. Design principles of photo-bioreactors for cultivation of microalgae. Eng. Life Sci. **9**:165–177.
27. **Radakovits R, Jinkerson RE, Darzins A, Posewitz MC.** 2010. Genetic engineering of algae for enhanced biofuel production. Eukaryot. Cell **9**:486–501.

28. **Richardson JW, Outlaw JL, Allison M.** 2010. The economics of microalgae oil. AgBioForum **13**:2.
29. **Sahin-Toth M, Frillingos S, Lengeler JW, Kaback HR.** 1995. Active transport by the CscB permease in Escherichia coli K-12. Biochem. Biophys. Res. Commun. **208**:1116–1123.
30. **Salerno GL, Curatti L.** 2003. Origin of sucrose metabolism in higher plants: when, how and why? Trends Plant Sci. **8**:63–69.
31. **Sheehan J, Dunahay T, Benemann J, Roessler P.** 1998. Look back at the U.S. Department of Energy's aquatic species program: biodiesel from algae. Close-out report NREL/TP-580-24190. National Renewable Energy Laboratory, Golden, CO.
32. **Shetty RP, Endy D, Knight TF, Jr.** 2008. Engineering BioBrick vectors from BioBrick parts. J. Biol. Eng. **2**:5.
33. **Sims R, Taylor M.** 2008. From 1st to 2nd generation biofuel technologies. IEA, Paris, France.
34. **Somerville C, Youngs H, Taylor C, Davis SC, Long SP.** 2010. Feedstocks for lignocellulosic biofuels. Science **329**:790–792.
35. **Stenbaek A, Jensen PE.** 2010. Redox regulation of chlorophyll biosynthesis. Phytochemistry **71**:853–859.
36. **Suzuki E, et al.** 2010. Carbohydrate metabolism in mutants of the cyanobacterium Synechococcus elongatus PCC 7942 defective in glycogen synthesis. Appl. Environ. Microbiol. **76**:3153–3159.
37. **Timilsina GR, Beghin JC, van der Mensbrugghe D, Mevel S.** 2010. The impacts of biofuel targets on land-use change and food supply. The World Bank Development Research Group, Washington, DC.
38. **Vadyvaloo V, Smirnova IN, Kasho VN, Kaback HR.** 2006. Conservation of residues involved in sugar/H(+) symport by the sucrose permease of Escherichia coli relative to lactose permease. J. Mol. Biol. **358**:1051–1059.
39. **Waclawovsky AJ, Sato PM, Lembke CG, Moore PH, Souza GM.** 2010. Sugarcane for bioenergy production: an assessment of yield and regulation of sucrose content. Plant Biotechnol. J. **8**:263–276.
40. **Wilson KE, Ivanov AG, GÖquist Grodzinski B, Sarhan F, Huner NPA.** 2006. Energy balance, organellar redox status, and acclimation to environmental stress. Can. J. Bot. **84**:1355–1370.
41. **Wu L, Birch RG.** 2007. Doubled sugar content in sugarcane plants modified to produce a sucrose isomer. Plant Biotechnol. J. **5**:109–117.
42. **Zhang F, Rodriguez S, Keasling JD.** 2011. Metabolic engineering of microbial pathways for advanced biofuels production. Curr. Opin. Biotechnol.
43. **Zhu XG, Long SP, Ort DR.** 2010. Improving photosynthetic efficiency for greater yield. Annu. Rev. Plant Biol. **61**:235–261.
44. **Zhu XG, Long SP, Ort DR.** 2008. What is the maximum efficiency with which photosynthesis can convert solar energy into biomass? Curr. Opin. Biotechnol. **19**:153–159.